



## Enhanced Ammonia-Borane Decomposition by synergistic catalysis using CoPd nanoparticles supported on titano-silicates

Received 00th January 20xx,  
Accepted 00th January 20xx

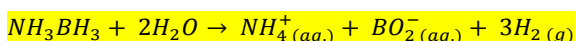
Jaime García-Aguilar<sup>a</sup>, Miriam Navlani-García<sup>b</sup>, Ángel Berenguer-Murcia<sup>a</sup>, Kohsuke Mori<sup>b</sup>,  
Yasutaka Kuwahara<sup>b</sup>, Hiromi Yamashita<sup>b,\*</sup>, Diego Cazorla-Amorós<sup>a,\*</sup>

DOI: 10.1039/x0xx00000x

www.rsc.org/

Pd and Co<sub>x</sub>Pd<sub>1-x</sub> nanoparticles (NPs) synthesized by the reduction by solvent method were loaded on SiO<sub>2</sub> and Ti-SiO<sub>2</sub> supports and the resulting catalysts were tested in the ammonia-borane decomposition reaction under dark and UV-Vis conditions. The synergistic promotion of Co (in the NPs) and Ti (in the support) combined with the UV-Vis light irradiation enhanced the catalytic activity showing very promising TOFs values (from 1.53 to 49.5 mol H<sub>2</sub>·mol Pd<sup>-1</sup>·min<sup>-1</sup>) in this kind of catalysts.

The decomposition of small molecules (such as formic acid or ammonia-borane (AB)) is one of the most promising alternatives for the in-situ H<sub>2</sub> generation towards a H<sub>2</sub> scenario implementation.<sup>1-3</sup> AB is claimed as one of the inorganic compounds with the highest hydrogen content (19.6 H<sub>2</sub> wt. %). This, added to its high reactivity with noble metals (such as Ru, Pd or Pt) makes it one of the best candidates for its use as H<sub>2</sub> feed in a PEMFC.<sup>3-8</sup> The total decomposition of this compound in liquid phase using water as solvent produces 3 mol of H<sub>2</sub> per mol of AB according to the following reaction equation.<sup>9</sup>



Ammonia borane is a liquid-phase chemical hydrogen storage material with great current interest. Its decomposition on a wide range of catalysts has been extensively reported in the literature. Among these, noble metals such as Rh, Ir, Ru, and Pt, have shown interesting catalytic activities,<sup>10</sup> but they are unsuitable for widespread practical applications due to their availability and price. Previous studies have demonstrated that bimetallic nanoparticles combining a noble metal and a first-

row transition metal forming an alloy structure could be promising candidates for the design of catalysts for the hydrolysis of ammonia borane.<sup>11</sup> In order to assess the beneficial effect of these noble metal/first-row transition metal combinations for this application, we have used Pd due to its moderate activity among noble metals<sup>12</sup> and Co because it shows the highest activity among non-noble metal catalysts.<sup>11,13,14</sup>

The enhancement of the catalytic activity of the supported noble metal can be attained by different routes; i) increasing the metal dispersion on the support by the synthesis of very small NPs,<sup>15</sup> ii) alloying the noble metal with a transition metal, (which is also attractive due to the cost reduction of the catalysts)<sup>11,16,17</sup> and iii) supporting the NPs on an UV-Vis active support to upgrade the electron-transfer from the support to the NPs.<sup>1,18</sup> In the present study, the synthesis of Pd and Co-Pd NPs by the reduction-by-solvent methodology has been applied with successful results in the production of H<sub>2</sub> by AB decomposition. The synthesis conditions allow a perfect control over size and morphology of the NPs (both mono- and bimetallic). Pure or alloyed cobalt (as oxide or reduced form) has been addressed in the recent literature as a promising metal in the AB decomposition reaction due to its low cost (compared with noble metals) and its high activity in relevant reactions.<sup>12,16,19-21</sup> Due to their different reduction potential (compared with Pd), when M-Pd (i. e. Cu or Co) are well-alloyed there is a charge transfer from the M to Pd increasing the electron density on the Pd atom and its activity in the AB decomposition is enhanced.<sup>1,18</sup> On the other hand, the use of an active support (under UV-Vis conditions), such as titania or a titano-silicate (Ti-SiO<sub>2</sub>), is an available strategy to enhance the catalytic activity of the final catalytic system.<sup>22,23</sup>

In the present work, Pd and Co<sub>x</sub>Pd<sub>1-x</sub> NPs were prepared by the well-established procedure of the reduction by solvent method using PVP as capping agent and following an already reported procedure.<sup>15,24</sup> After their purification, the NPs were loaded on SiO<sub>2</sub> and Ti-SiO<sub>2</sub> (UV-Vis inactive and active supports, respectively) to study their catalytic activity in AB

<sup>a</sup> Materials Science Institute and Inorganic Chemistry Department, Alicante University, Ap. 99, E-03080 Alicante, Spain. \* (e-mail: [cazorla@ua.es](mailto:cazorla@ua.es))

<sup>b</sup> Division of Materials and Manufacturing Science, Graduate School of Engineering, Osaka University, 2-1 Yamada-oka, Suita, Japan. \* (e-mail: [yamashita@mat.eng.osaka-u.ac.jp](mailto:yamashita@mat.eng.osaka-u.ac.jp))

† Footnotes relating to the title and/or authors should appear here.

Electronic Supplementary Information (ESI) available: [details of any supplementary information available should be included here]. See DOI: 10.1039/x0xx00000x

decomposition in liquid-phase reaction (see all the experimental details in the SI).

From the textural characterization of the catalysts (see SI) it must be mentioned that there were no significant changes in the isotherm shape and specific surface properties between the two raw supports ( $\text{SiO}_2$  and  $\text{Ti-SiO}_2$ ) and the resulting catalysts after NPs impregnation. Regarding the NPs preparation and deposition on the supports two main characteristics must be highlighted: both the nominal Co/Pd ratio and the nominal metal loading (1 wt. %) were approximately achieved in all the catalysts (calculated from ICP-OES results). For the two series of samples ( $\text{SiO}_2$  and  $\text{Ti-SiO}_2$ -based catalysts) the NPs size was very similar for both samples upon deposition on the supports (3.4–3.5 nm, see TEM micrographs and histograms in Fig. 1). Therefore, any change in the catalytic activity may be ascribed to the chemical composition of the supports or modifications in the NPs size with respect to the monometallic counterpart. From CO adsorption experiments after  $\text{H}_2$  pre-reduction of the catalysts it is possible to obtain information about the Co and Pd distribution in the bimetallic NPs. To this end the adsorbed CO moles were normalized per mol of Pd and per total mol of metal (Co and Pd) (see SI). The Pd-normalized results showed an approximate constant CO adsorption of about 0.23 mol CO/mol Pd, while for the total metal adsorption, the adsorbed CO decreased proportionally as the Co content in the NPs increased. These results together with the surface Co/Pd ratio determined by XPS analysis might confirm the homogeneous distribution of both elements in the alloyed NPs structures. In order to study the UV-Vis light response, the solid UV-Vis analysis was mandatory (see SI).  $\text{SiO}_2$  did not present any absorption and in the raw  $\text{Ti-SiO}_2$  a small fraction of octahedral Ti(IV) was observed at 300 nm but the main absorption of the support was displayed in the 200 nm range corresponding to tetrahedral Ti(IV) dispersed in the  $\text{SiO}_2$  framework.<sup>25,26</sup> After NPs loading on the supports a broad absorption at around 300 nm was observed even in the  $\text{SiO}_2$ -based catalysts due to the Pd NPs absorption.<sup>27</sup>

Pd, Co and Ti XPS analysis offered information about the electronic state of these elements in order to determine the influence of the Co presence in the NPs and the incorporation of the Ti in the support. Binding Energy (BE) values as well as the most relevant peaks of their corresponding XPS spectra are presented in Table S1. In all catalysts the signals corresponding to Pd(0) and  $\text{Pd}^{\delta+}$  could be clearly observed. The appearance of this latter signal is due to the electron deficient Pd which may be Pd directly interacting with PVP. Cobalt species (such as electron deficient Co or  $\text{CoO}_x$ ) and also electron deficient Ti(IV) due to its dispersion into the  $\text{SiO}_2$  support are also observed in the  $\text{Co}_x\text{Pd}_{1-x}/\text{Ti-SiO}_2$  catalysts. In this respect, it must be noted that evidence of the presence of Co(0) (778.0 eV) was not found in our analysis.<sup>26,28</sup>

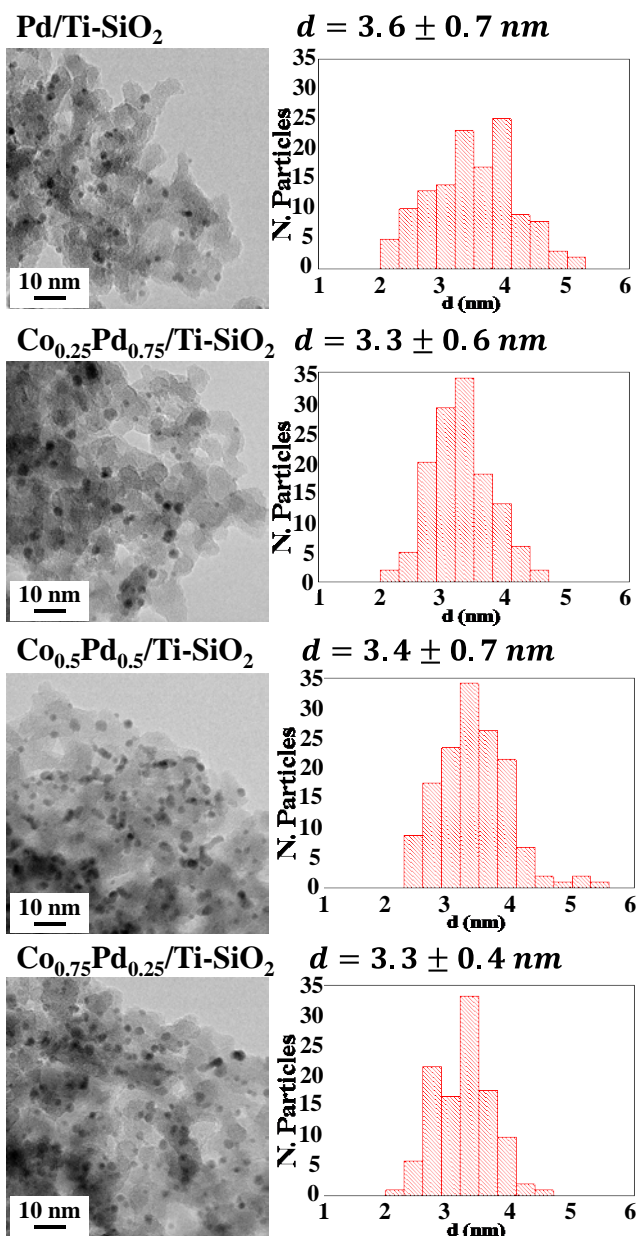


**Fig 1.**  $\text{Co}_x\text{Pd}_{1-x}$  NPs deposited on  $\text{Ti-SiO}_2$  TEM images and their corresponding histograms and average particle size.

For the  $\text{SiO}_2$ -based catalysts a slight decrease in the XPS Pd(0) and  $\text{Pd}^{\delta+}$  BE was observed when Co was incorporated into the NPs due to the Pd electron density enrichment. An increase in Pd(0) % content due to the addition of the Co was also observed, from 73.7 % for Pd/ $\text{SiO}_2$  to 86.0 and 83.5 % for  $\text{Co}_{0.25}\text{Pd}_{0.75}$  and  $\text{Co}_{0.5}\text{Pd}_{0.5}/\text{SiO}_2$ , respectively. However, when the Co content increased to  $\text{Co}_{0.75}\text{Pd}_{0.25}/\text{SiO}_2$  the Pd(0) content decreased to 69.6 %. This fact might be due to the presence of the different Co species in the NPs. Thus, according to these results it seems that for low Co contents (i.e.  $\text{Co}_{0.25}\text{Pd}_{0.75}$  and  $\text{Co}_{0.5}\text{Pd}_{0.5}$ ) there is an efficient charge transfer from the Co species to Pd which it is in good agreement with the absence of metallic Co signals in the XPS spectra, but when the Co ratio increases, more oxidized Co species are formed and the charge

transfer is hindered. Furthermore the PVP-Metal interaction and its effect on the final electronic features of the resulting NPs should also be considered. Along this line, the high surface PVP/Pd ratio in the  $\text{Co}_{0.75}\text{Pd}_{0.25}$  NPs together with the strong PVP-Pd interaction and the electron-withdrawing property of PVP through the C=O groups<sup>29,30</sup>, might also be responsible for the higher  $\text{Pd}^{\delta+}$  content detected in  $\text{Co}_{0.75}\text{Pd}_{0.25}/\text{SiO}_2$ .

On the other hand, the Pd(0) signal was shifted 0.3 eV to higher BE values when the Pd NPs were deposited on the Ti-SiO<sub>2</sub> support and reduced its respective  $\text{Pd}^{\delta+}$  content. This modification is in good agreement with the Ti 2p(3/2) BE displacement from 460.48 eV (in the raw support) to 459.38 eV (after the NPs loading).<sup>26,31</sup> This observation confirms a charge transfer from the Pd NPs to the Ti-based support. Regarding the Pd BE modifications in  $\text{Co}_x\text{Pd}_{1-x}$  NPs when Ti-SiO<sub>2</sub> was used as support there was also a decrease of the BE at which the peaks appeared as well as an increase of the Pd(0) content (higher in value than the SiO<sub>2</sub>-catalysts, although for high Co loadings this trend is no longer observed, vide supra) and the Ti(IV) BE is significantly reduced to 458.93 when the  $\text{Co}_{0.25}\text{Pd}_{0.75}$  NPs were deposited. For this catalyst series, the same trend was observed in Pd(0) content when the Co ratio increased in the NPs.

The catalysts were studied in the AB decomposition reaction, using a metal/AB molar ratio of 0.02 and analyzing the production of H<sub>2</sub> every 2.5 min (see full details of the procedure in the SI). The H<sub>2</sub> evolution profiles indicated that no induction period was necessary but important differences in the catalytic activities were observed. For the least active catalyst total AB conversion was achieved after approximately 25 minutes of reaction while for the most active samples less than 10 minutes were necessary (results of the AB conversions in terms of  $n(\text{H}_2)/n(\text{AB})$  ratios are shown in the SI). To compare the activity of all the prepared catalysts the TOFs values (at 2.5 min.) under dark and UV-Vis light conditions were calculated (with respect to Pd and total metal content) and presented in Fig. 2. It must be noted that when the supports were used without any nanoparticles impregnated on their surface, no or negligible activity in the AB decomposition reaction was observed.

As the Co ratio increased in the NPs supported on SiO<sub>2</sub> (Fig. 2A) the specific activity of the Pd increased proportionally to the Co content from their initial value of 1.5 to 34.4 ( $\text{mol H}_2 \cdot \text{mol Pd}^{-1} \cdot \text{min}^{-1}$ ) measured under dark conditions. This behavior was in good agreement with the XPS results and other reported works, where the electron enrichment of the noble metal (as Pd) from a transition metal (such as Ni or Cu) was studied<sup>24,32</sup>. However, when the catalysts supported on SiO<sub>2</sub> were tested under UV-Vis irradiation a small decrease of the activity was obtained. This activity loss can be assigned to the partial degradation of PVP and subsequent Pd sites blocking on the NPs surface under UV-Vis light irradiation.<sup>33</sup> For the same catalytic tests but considering Co content for the TOF calculation (Fig. 2B), there was a maximum in the activity (for the nominal  $\text{Co}_{0.5}\text{Pd}_{0.5}$  NPs) of 13.9 ( $\text{mol H}_2 \cdot \text{mol M}^{-1} \cdot \text{min}^{-1}$ ).

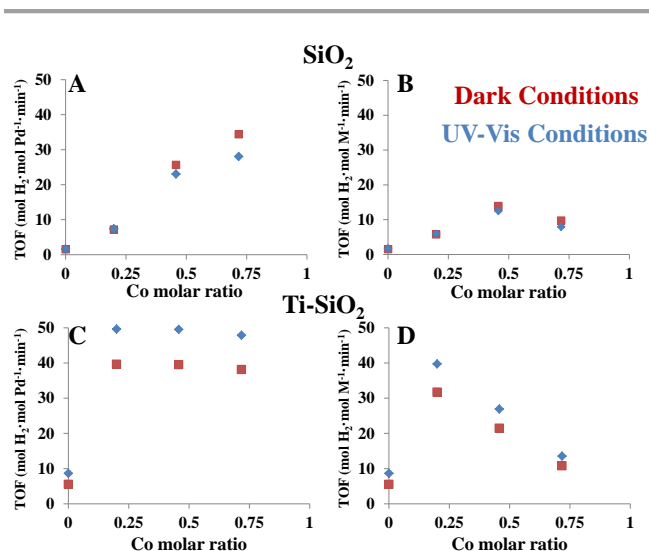


**Fig. 2.** TOFs values based on Pd and M (Pd and Co) vs Co molar ratio for AB decomposition under dark and UV-Vis light irradiation conditions. A) and B) results presented for the catalysts prepared using SiO<sub>2</sub> as support, C) and D) when Ti-SiO<sub>2</sub> is used as support.

Regarding the catalytic behavior of Ti-SiO<sub>2</sub>-based catalysts (Fig. 2C and 2D) a noticeable enhancement in the catalytic activity with respect to the SiO<sub>2</sub> samples was obtained for all catalysts under both conditions (dark and UV-Vis). Even for the pure Pd based catalysts under dark conditions, there is a considerable increase from 1.5 to 5.5 in the TOF value ( $\text{mol H}_2 \cdot \text{mol Pd}^{-1} \cdot \text{min}^{-1}$ ) when the Ti is incorporated to the support. In this sense, the Ti-based silicate catalysts might present strong interactions between TiO<sub>2</sub>-based supports and AB which favors its decomposition as previously reported.<sup>34,35</sup> Comparing the Pd-normalized catalysts results, the TOF drastically increased from 5.5 for the Pd/Ti-SiO<sub>2</sub> catalysts to ~40 (approximately) for any Co content. In addition to this increase the Pd-normalized activity of the samples increased up to 49.5 ( $\text{mol H}_2 \cdot \text{mol Pd}^{-1} \cdot \text{min}^{-1}$ ) when the catalysts were tested under UV-Vis light irradiation. On the other hand, for the total metal normalized TOFs, the highest value was obtained for  $\text{Co}_{0.25}\text{Pd}_{0.75}/\text{Ti-SiO}_2$  with a TOF value of 31.7 and 39.7 ( $\text{mol H}_2 \cdot \text{mol M}^{-1} \cdot \text{min}^{-1}$ ) under dark and UV-Vis light conditions, respectively. Upon consideration of these catalytic tendencies, it seems that under UV-Vis light irradiation conditions the activity per Pd content in this kind of catalysts ( $\text{Co}_x\text{Pd}_{1-x}/\text{Ti-SiO}_2$ ) is the same regardless of the Co content ( $49.5 \text{ mol H}_2 \cdot \text{mol Pd}^{-1} \cdot \text{min}^{-1}$ ) corroborating the synergistic effect of Co (alloyed in the NPs) and, specially, Ti (incorporated into the support). In this respect, the role of the Ti photocatalytic enhancement due to the accumulation of electrons and holes in the metal deposited on its surface and their transfer to the AB molecules enhancing their catalytic decomposition has already been reported recently.<sup>36</sup>

In Fig. 3 the H<sub>2</sub> production ( $\mu\text{mol}$ ) after 2.5 minutes of reaction with the Ti-SiO<sub>2</sub> based catalysts under dark and UV-Vis light conditions are shown. As it can be observed there was a

general positive effect of the UV-Vis light irradiation in the H<sub>2</sub> production for all samples under study. However, the outstanding enhancement displayed by the Co<sub>0.25</sub>Pd<sub>0.75</sub>/Ti-SiO<sub>2</sub> catalyst should be pointed out. This paramount catalytic behavior confirms the suitability of the present catalytic system and makes it a promising candidate for its possible implementation in H<sub>2</sub>-fed devices.

The results in TOF and AB conversion to H<sub>2</sub> production for the Co<sub>0.25</sub>Pd<sub>0.75</sub>/Ti-SiO<sub>2</sub> under UV-Vis light are lower compared with highly complex silica-coated cobalt ferrite loaded with Pd NPs <sup>20</sup> yet higher compared to related works that also use Co-Pd based catalysts and also similar metal/AB ratio <sup>11,37,38</sup> using high performance carbon materials and significantly higher metal loadings.

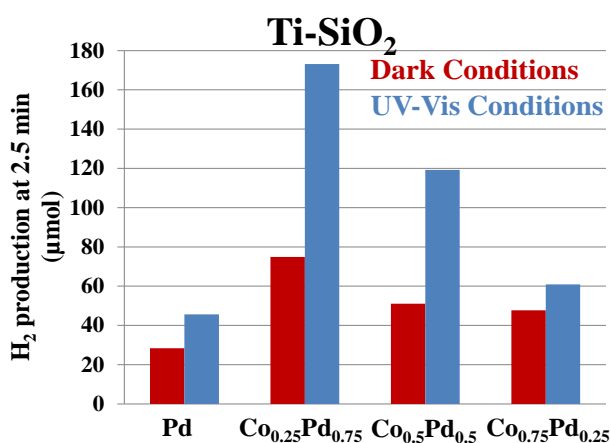


**Fig. 3.** H<sub>2</sub> production (μmol) of the Ti-based catalysts after 2.5 minutes of reaction under dark and UV-Vis irradiation conditions.

## Conclusions

In summary, highly active catalysts with less than 1 wt. % of noble metal content for AB decomposition were synthesized taking advantage of the twofold promotion of the initial Pd/SiO<sub>2</sub> catalytic system; increasing the electron density of the Pd through its alloying with Co in the NPs and deposition of these NPs on a very simple and active UV-Vis-responsive support doped with Ti. As a result, a very promising TOF (49.5 mol H<sub>2</sub>·mol Pd<sup>-1</sup>·min<sup>-1</sup>) with a very fast H<sub>2</sub> delivery of more than 160 μmol of H<sub>2</sub> in less than 2.5 min has been obtained by AB decomposition using a sample containing only 0.8 wt. % of Pd. These promising catalysts benefit from the catalytic synergy between Pd and Co in the NPs that allows the electron density transfer from the Co to the Pd (as it is observed by XPS) on the one hand, and the incorporated Ti in the support (making it active to the UV-Vis radiation) when it is tested under UV-Vis irradiation conditions on the other hand.

## Acknowledgements

We thank the Spanish Ministry of Economy and Competitiveness (MINECO), Generalitat Valenciana and FEDER (Projects CTQ2015-66080-R MINECO/FEDER and PROMETEOII/2014/010) for financial support. J.G.A. thanks the MINECO for his fellowship (BES-2013-063678) and specially thanks the mobility grant of MINECO (EEBB-I-15-10219) at Osaka University.

## Notes and references

- H. Cheng, T. Kamegawa, K. Mori, and H. Yamashita, *Angew. Chem. Int. Ed. Engl.*, 2014, **53**, 2910–4.
- K. Mori, M. Dojo, and H. Yamashita, *ACS Catal.*, 2013, **3**, 1114–1119.
- K. Mori, K. Miyawaki, and H. Yamashita, *ACS Catal.*, 2016, **6**, 3128–3135.
- S. Enthaler, J. von Langermann, and T. Schmidt, *Energy Environ. Sci.*, 2010, **3**, 1207–1217.
- C. W. Hamilton, R. T. Baker, A. Staubitz, and I. Manners, *Chem. Soc. Rev.*, 2009, **38**, 279–293.
- F. H. Stephens, V. Pons, and R. Tom Baker, *Dalton Trans.*, 2007, **2**, 2613–26.
- Z.-L. Wang, J.-M. Yan, Y. Ping, H.L. Wang, W.-T. Zheng, and Q. Jiang, *Angew. Chemie Int. Ed.*, 2013, **52**, 4406–4409.
- U. Eberle, M. Felderhoff, and F. Schüth, *Angew. Chemie Int. Ed.*, 2009, **48**, 6608–6630.
- T. Kamegawa and T. Nakae, *Chem. Commun.*, 2015, **51**, 16802–16805.
- M. Yadav and Q. Xu, *Energy Environ. Sci.*, 2012, **5**, 9698.
- D. Sun, V. Mazumder, Ö. Metin, and S. Sun, *ACS Nano*, 2011, **5**, 6458–6464.
- Ö. Metin, Ş. Şahin, and S. Özkaz, *Int. J. Hydrogen Energy*, 2009, **34**, 6304–6313.
- J.-M. Yan, X.-B. Zhang, H. Shioyama, and Q. Xu, *J. Power Sources*, 2010, **195**, 1091–1094.
- Ö. Metin and S. Özkaz, *Int. J. Hydrogen Energy*, 2011, **36**, 1424–1432.
- S. Domínguez-Domínguez, Á. Berenguer-Murcia, D. Cazorla-Amorós, and Á. Linares-Solano, *J. Catal.*, 2006, **243**, 74–81.
- J.-M. Yan, X.-B. Zhang, T. Akita, M. Haruta, and Q. Xu, *J. Am. Chem. Soc.*, 2010, **132**, 5326–5327.
- D. Sun, V. Mazumder, Ö. Metin, and S. Sun, *ACS Catal.*, 2012, **2**, 1290–1295.
- Y. Kuwahara, K. Nishizawa, T. Nakajima, T. Kamegawa, K. Mori, and H. Yamashita, *J. Am. Chem. Soc.*, 2011, **133**, 12462–12465.
- J. Hu, Z. Chen, M. Li, X. Zhou, and H. Lu, *ACS Appl. Mater. Interfaces*, 2014, **6**, 13191–200.
- S. Akbayrak, M. Kaya, M. Volkan, and S. Özkaz, *Appl. Catal. B Environ.*, 2014, **147**, 387–393.
- A. Rossin and M. Peruzzini, *Chem. Rev.*, 2016, **116**, 8848–8872.
- F. X. Llabrés i Xamena, P. Calza, C. Lamberti, C. Prestipino, A. Damin, S. Bordiga, E. Pelizzetti, and A. Zecchina, *J. Am. Chem. Soc.*, 2003, **125**, 2264–2271.

23. Y. Shiraishi, N. Saito, and T. Hirai, *J. Am. Chem. Soc.*, 2005, **127**, 8304–8306.
24. J. García-Aguilar, I. Miguel-García, Á. Berenguer-Murcia, and D. Cazorla-Amorós, *Carbon*, 2014, **66**, 599–611.
25. A. Prieto, M. Palomino, U. Díaz, and A. Corma, *Catal. Today*, 2014, **227**, 87–95.
26. A. K. Sinha, S. Seelan, S. Tsubota, and M. Haruta, *Angew. Chemie Int. Ed.*, 2004, **43**, 1546–1548.
27. M. Navlani-García, K. Mori, M. Wen, Y. Kuwahara, and H. Yamashita, *Bull. Chem. Soc. Jpn.*, 2015, **88**, 1500–1502.
28. A. Bulut, M. Yurderi, İ. E. Ertas, M. Celebi, M. Kaya, and M. Zahmakiran, *Appl. Catal. B Environ.*, 2016, **180**, 121–129.
29. Y. Borodko, S. M. Humphrey, T. D. Tilley, H. Frei, and G. A. Somorjai, *J. Phys. Chem. C*, 2007, **111**, 6288–6295.
30. I. Miguel-García, Á. Berenguer-Murcia, and D. Cazorla-Amorós, *Appl. Catal. B Environ.*, 2010, **98**, 161–170.
31. M. C. Capel-Sanchez, G. Blanco-Brieva, J. M. Campos-Martin, M. P. de Frutos, W. Wen, J. A. Rodriguez, and J. L. G. Fierro, *Langmuir*, 2009, **25**, 7148–7155.
32. K. Mori, H. Tanaka, M. Dojo, K. Yoshizawa, and H. Yamashita, *Chem. - A Eur. J.*, 2015, **21**, 12085–12092.
33. C. Aliaga, J. Y. Park, Y. Yamada, H. S. Lee, C. Tsung, P. Yang, and G. a Somorjai, *J. Phys. Chem. C*, 2009, **113**, 6150–6155.
34. O. V. Komova, V. I. Simagina, N. L. Kayl, G. V. Odegova, O. V. Netskina, Y. A. Chesalov, and A. M. Ozerova, *Int. J. Hydrogen Energy*, 2013, **38**, 6442–6449.
35. R. Fernandes, N. Patel, A. Miotello, R. Jaiswal, and D. C. Kothari, *Int. J. Hydrogen Energy*, 2012, **37**, 2397–2406.
36. A. Yousef, N. A. M. Barakat, and H. Y. Kim, *Appl. Catal. A Gen.*, 2013, **467**, 98–106.
37. J. Wang, Y.-L. Qin, X. Liu, and X.-B. Zhang, *J. Mater. Chem.*, 2012, **22**, 12468.
38. B. Kılıç, S. Şencanlı, and Ö. Metin, *J. Mol. Catal. A Chem.*, 2012, **361–362**, 104–110.